SUPPLEMENTARY INFORMATION FOR

N-terminal cleavage of Cyclophilin D boosts its ability to bind F-ATP Synthase

Gabriele Coluccino, Alessandro Negro, Antonio Filippi, Camilla Bean, Valentina Pia Muraca, Clarissa Gissi, Diana Canetti, Maria Chiara Mimmi, Elisa Zamprogno, Francesco Ciscato, Laura Acquasaliente, Vincenzo De Filippis, Marina Comelli, Michela Carraro, Andrea Rasola, Christoph Gerle, Paolo Bernardi, Alessandra Corazza and Giovanna Lippe

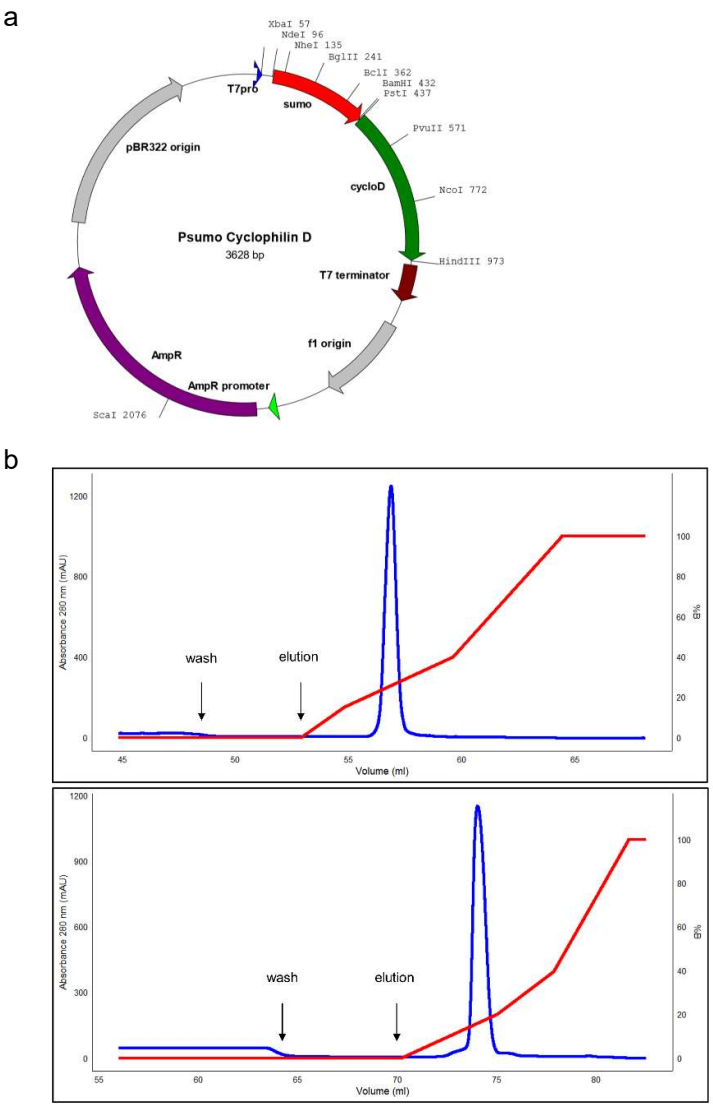

Supplementary Figure 1. **Recombinant protein purification details. a**. Schematic representation of the plasmid with which *E. coli* cells were transformed (cycloD corresponded either to the sequence of human FL-CyPD or ΔN-CyPD). **b**. Chromatograms of the cation exchange chromatography, the last step of protein purification. Blue trace: Absorbance at 280 nm. Red trace: FPLC solution B percentage.

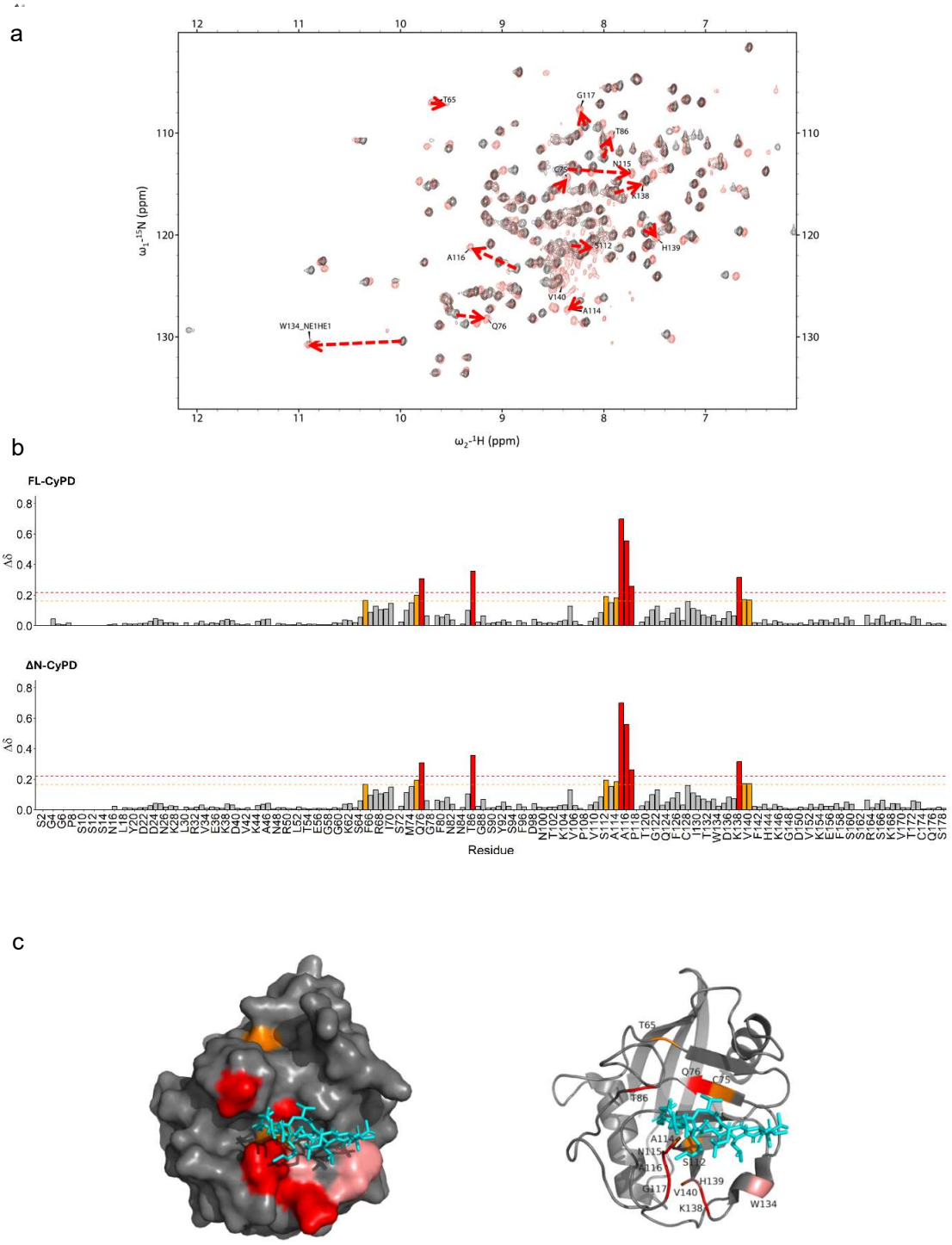

Supplementary Figure 2. **Cyclosporine A binding to FL-CyPD and ΔN-CyPD. a.** Representative HSQC spectra of FL-CyPD with (red spectrum) and without (black spectrum) 1:1 CsA. Significantly perturbed residues are presented. **b**. Chemical shift perturbation upon CsA binding. Bars are colored according to the CSP: red bars have a Δδ higher than $\overline{\Delta\delta} + 3\,sd$ (red dotted line), orange bars have a Δδ higher than $\overline{\Delta\delta} + 2\,sd$ (orange dotted line), grey bars are non-perturbed residues. **c.** CsA-bound CyPD (PDB ID: 2Z6W). Residues are coloured according to the CSP analysis showed in the upper panel. W134 and H139 are coloured in pink. See the main text for further details.

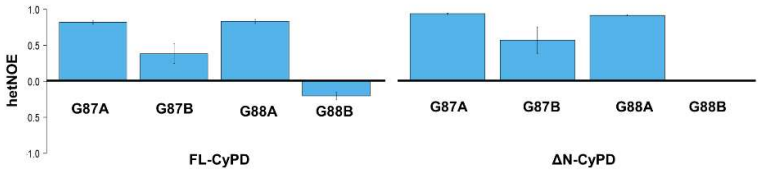

Supplementary Figure 3. **Residue flexibility in G88B and G87B of FL-CyPD and ΔN-CyPD.** Barplots representing the hetNOE for both forms of G88 and G87 of FL-CyPD (right) and ΔN-CyPD (left) are shown. Bars are coloured as in Figure 3 (blue=random coil).

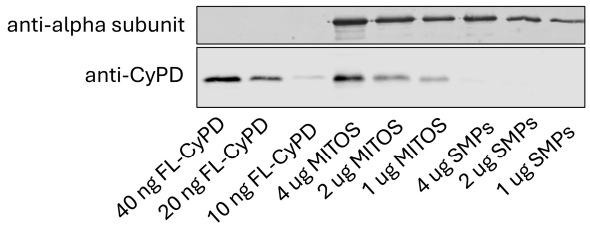

Supplementary Figure 4. **CyPD content of mitochondria and SMP preparations.** Western blot against CyPD or F-ATP Synthase subunit α of different quantities of recombinant FL-CyPD (lanes 1-3), pig heart mitochondria (lanes 4-6), and SMP prepared by mitochondria exposure to ultrasonic energy (lanes 7-9). The µg of protein loaded onto the gel are indicated. The figure shows that while endogenous CyPD was present in pig mitochondria, we were able to remove during the preparation of SMP, which are completely devoid of CyPD.

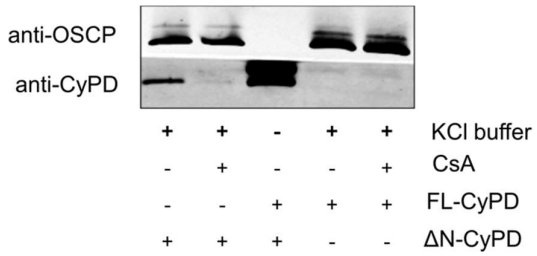

Supplementary Figure 5. **FL-CyPD binding to OSCP is undetectable in KCl buffer without phosphate.** Western blot against OSCP or CyPD of samples obtained from immunoprecipitation of OSCP from pig heart SMP incubated with 1 nmol CyP/mg SMP of either recombinant FL-CyPD or recombinant ΔN-CyPD with or without 2 μM CsA in KCl-based buffer not supplemented with phosphate.

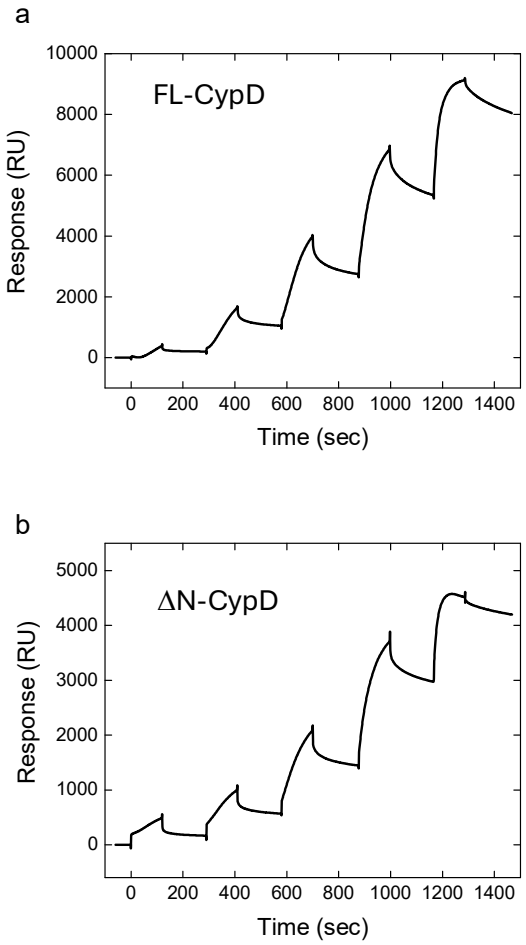

Supplementary Figure 6. **SPR analysis of CyPD binding to recombinant OSCP**. **a**. Sensograms were obtained by injecting increasing concentrations of FL-CyPD (**a**) and ΔN-CyPD (**b**) in the mobile phase, composed of 10mM Tris-HCl, pH7.4, containing 125mM KCl and 10mM potassium phosphate. SPR measurements were performed at 25°C in the single-cycle mode on a Biacore X-100 dual flow-cell instrument, after base line correction. Analysis of the sensograms was performed using the BIAevaluation software, within the framework of the single-site binding model, to extract k_{on}, k_{off} and K_d values, as follows: FL-CyPD, k_{on} = 467.1±8.6 M^{-1} s^{-1}; k_{off} = (5.66 ± 0.55) $\cdot 10^{-4}$ s^{-1}; K_d = (1.21±0.14)$\cdot 10^{-6}$ M. ΔN-CyPD: , k_{on} = (1.36± 0.26) $\cdot 10^{4}$ M^{-1} s^{-1}; k_{off} = (1.79± 0.56) $\cdot 10^{-4}$ s^{-1}; K_d = (1.31±0.66)$\cdot 10^{-8}$ M.

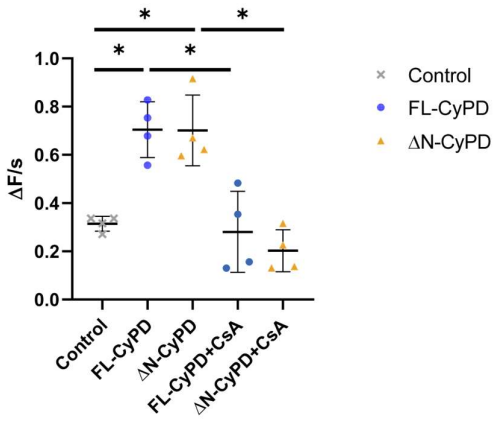

Supplementary Figure 7. **PPIase activity of recombinant FL-CyPD and ΔN-CyPD in KCl**. PPiase activity was assessed monitoring the intrinsic fluorescence of RNase T1 during its refolding in a buffer supplemented with 150 mM KCl with or without 1:10 CsA. Slopes of the linear part of the traces were interpolated and used as a probe of FL-CyPD or ΔN-CyPD catalytic activity. Data were analysed according to the Kruskal-Wallis test followed by Dunn's multiple comparisons test. (*$p < 0.05$).

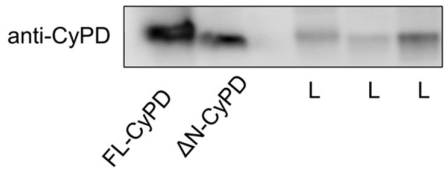

Supplementary Figure 8. **FL-CyPD and ΔN-CyPD cannot be separated by electrophoresis with commercial SDS-PAGE gels**. Western blot against CyPD of recombinant FL-CyPD and ΔN-CyPD and of three total lysate (L) samples separated on a commercial 0-20 gradient SDS-PAGE gel. The two proteins, FL-CyPD and ΔN-CyPD, were completely indistinguishable from one another.

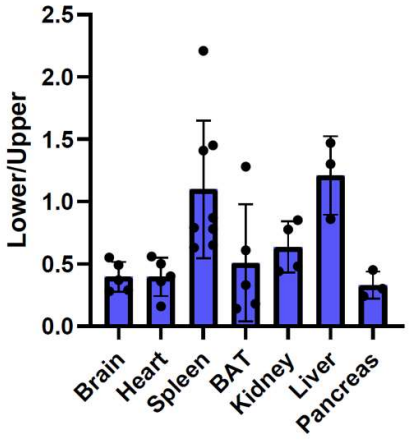

Supplementary Figure 9. **The ratio between lower and upper bands is tissue-specific**. Quantification of the ratio between the lower (~18 kDa) and upper (~19 kDa) bands responding to anti-CyPD antibodies in different murine tissues (see main text for further details).

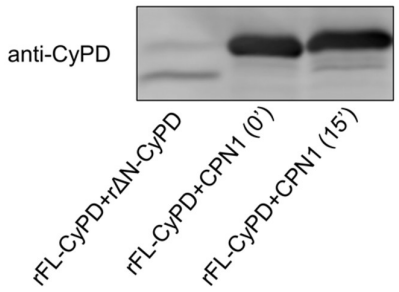

Supplementary Figure 10. **Western blot identification of FL-CyPD cleavage product**. Western blot against anti-CyPD before (second lane) and after (third lane) an incubation of 15 minutes between FL-CyPD and recombinant calpain-1. Recombinant FL-CyPD and ΔN-CyPD (first lane) were used as reference to assess their electrophoretic separation.

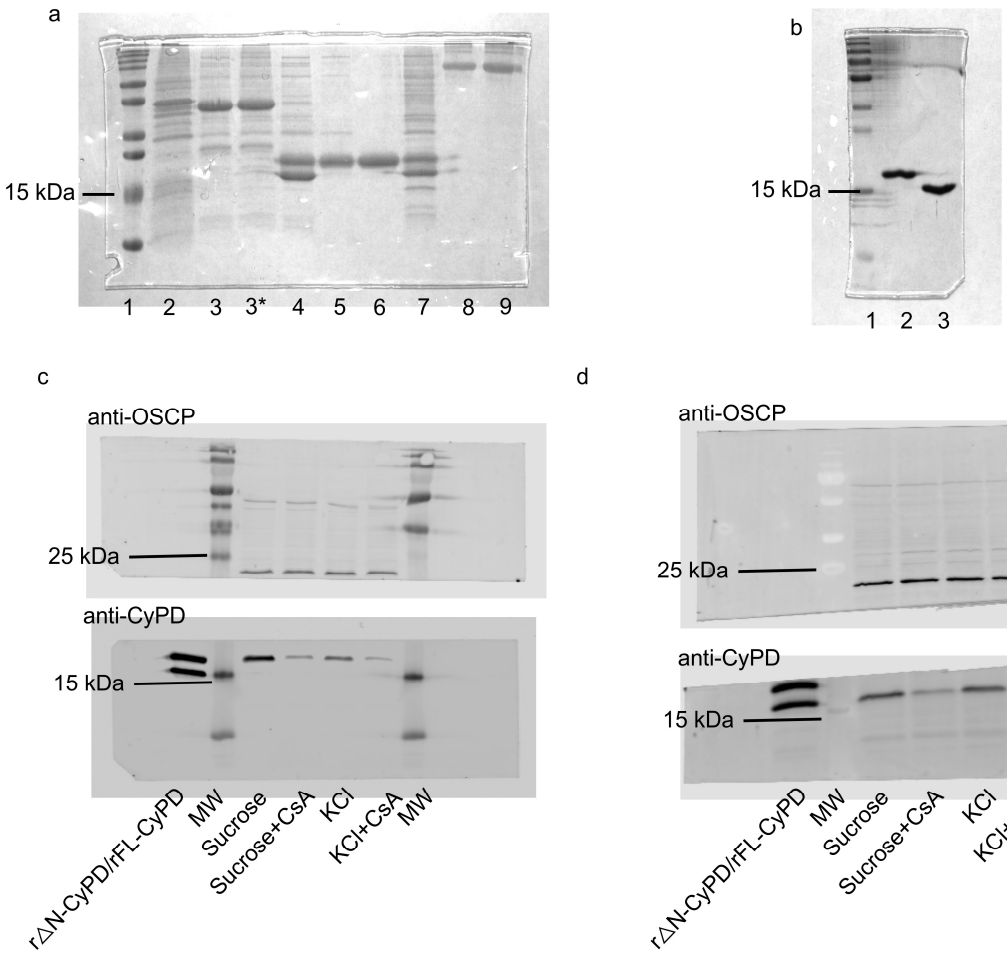
a
15 kDa
1 2 3 3* 4 5 6 7 8 9
b
15 kDa
1 2 3
c
anti-OSCP
25 kDa
anti-CyPD
15 kDa
rΔN-CyPD/rFL-CyPD
MW
Sucrose
Sucrose+CsA
KCl
KCl+CsA
MW
d
anti-OSCP
25 kDa
anti-CyPD
15 kDa
rΔN-CyPD/rFL-CyPD
MW
Sucrose
Sucrose+CsA
KCl
KCl+CsA
MW
e
anti-alpha subunit
70 kDa
50 kDa
anti-CyPD
25 kDa
rFL-CyPD
rΔN-CyPD
MW
BAT
Heart
Liver
Spleen
Pancreas
Brain
MW

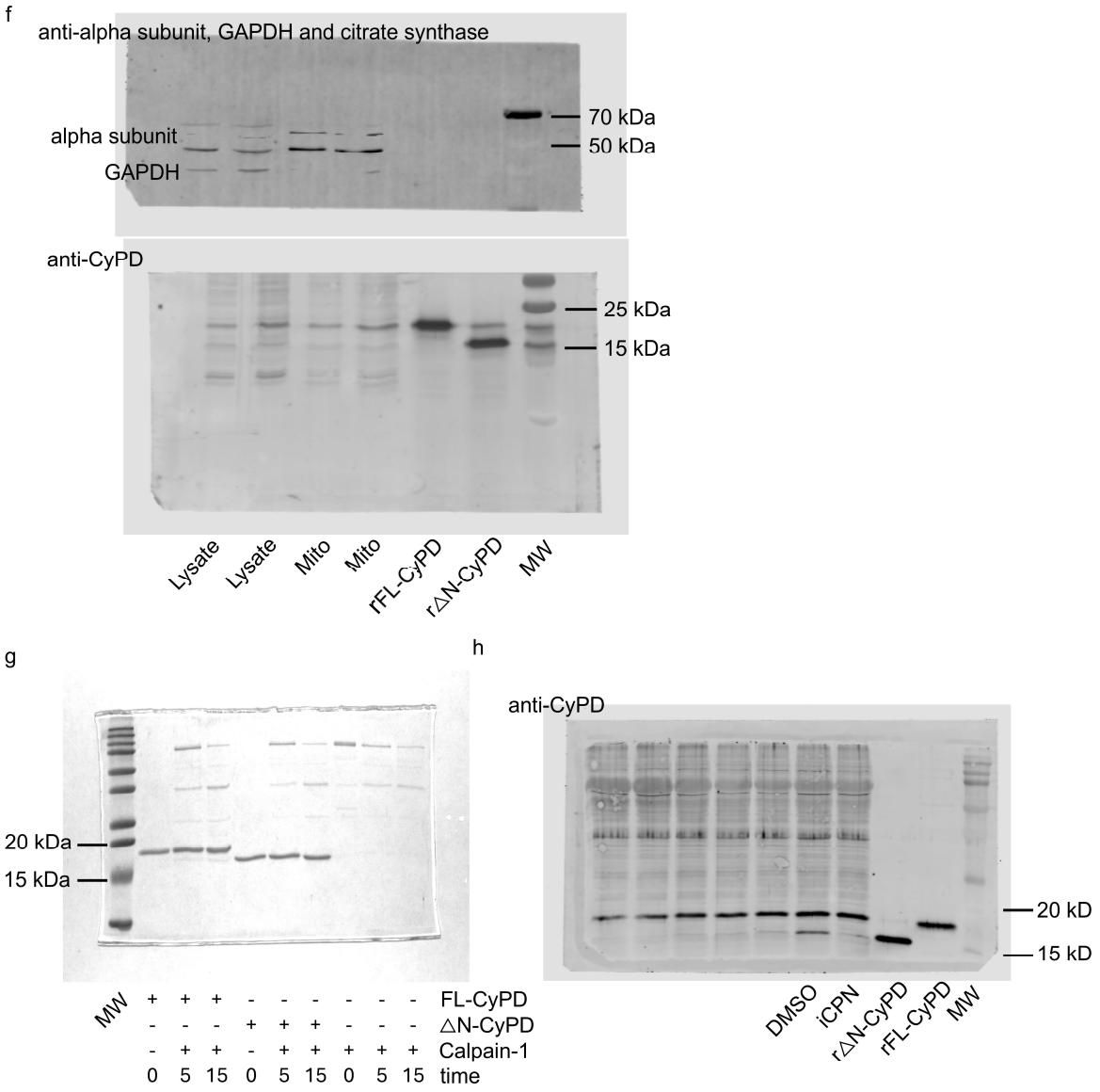

Supplementary Figure 11. **Original Coomassie-stained gels and immunoblots referenced in the main text. a**. Original Coomassie-stained gel corresponding to Fig. 1b. Lanes 1–8 match those in the main figure, with lane 3* representing a technical replicate of lane 3. Lanes 8 and 9 contain 2 µg and 4 µg of BSA, respectively, for quantification. **b**. Original Coomassie-stained gel corresponding to Fig. 1c. **c** Original immunoblots from Fig. 4a (FL-CyPD). In addition to the data presented in the main figure, recombinant FL-CyPD and ΔN-CyPD are shown in the first lane. **d.** Original immunoblot from Fig. 4a (ΔN -CyPD), with recombinant FL-CyPD and ΔN-CyPD also included in the first lane for comparison. **e**. Original immunoblots from Fig. 6a, with recombinant FL-CyPD and ΔN-CyPD displayed in the first and second lanes, respectively, compared to the main figure. **f.** Original immunoblots from Fig. 6b, featuring recombinant FL-CyPD and ΔN-CyPD in the first and second lanes, respectively. **g.** Original Coomassie-stained gel corresponding to Fig. 6f. **h.** Original immunoblot from Fig. 6g, with additional lanes present. Only those included in the main text figure are indicated.

Supplementary Table 1. **Temperature coefficients of G88 and G87 double forms.**

	FL-CyPD	ΔN-CyPD
G88A	-5.4 ppb	-5.2 ppb
G88B	-8.8 ppb	-8.8 ppb
G87A	-3.1 ppb	-3.1 ppb
G87B	-8.8 ppb	-10.5 ppb